Biotechnology Journal

DOI 10.1002/biot.200900004

Biotechnol. J. 2009, 4, 1168–1177

Research Article

Characterization of cell viability during bioprinting processes

Kalyani Nair[1], Milind Gandhi[1], Saif Khalil[1], Karen Chang Yan[2], Michele Marcolongo[3], Kenneth Barbee[4] and Wei Sun[1]

[1]Department of Mechanical Engineering and Mechanics, Drexel University, Philadelphia, PA, USA
[2]Department of Mechanical Engineering, The College of New Jersey, Ewing, NJ, USA
[3]Department of Materials Science and Engineering, Drexel University, Philadelphia, PA, USA
[4]School of Biomedical Engineering, Science & Health Systems, Drexel University, Philadelphia, PA, USA

Bioprinting is an emerging technology in the field of tissue engineering and regenerative medicine. The process consists of simultaneous deposition of cells, biomaterial and/or growth factors under pressure through a micro-scale nozzle. Cell viability can be controlled by varying the parameters like pressure and nozzle diameter. The process itself can be a very useful tool for evaluating an *in vitro* cell injury model. It is essential to understand the cell responses to process-induced mechanical disturbances because they alter cell morphology and function. We carried out analysis and quantification of the degree of cell injury induced by bioprinting process. A parametric study with different process parameters was conducted to analyze and quantify cell injury as well as to optimize the parameters for printing viable cells. A phenomenological model was developed correlating the percentage of live, apoptotic and necrotic cells to the process parameters. This study incorporates an analytical formulation to predict the cell viability through the system as a function of the maximum shear stress in the system. The study shows that dispensing pressure has a more significant effect on cell viability than the nozzle diameter. The percentage of live cells is reduced significantly (by 38.75%) when constructs are printed at 40 psi compared to those printed at 5 psi.

Received 9 January 2009
Revised 10 March 2009
Accepted 8 April 2009

Keywords: Bioprinting · Injury · Model · Regenerative medicine · Tissue engineering

1 Introduction

Tissue engineering and regenerative medicine is an interdisciplinary field that combines medicine and engineering to create a new knowledge base for engineering tissue constructs in applications such as drug delivery systems, pharmacokinetic devices for drug evaluation, animal on chip systems and organ replacements [1, 2]. However, the tissue-engineering community faces many challenges including cell sourcing, optimization of scaffold design, and processes for creating 3-D functional tissue constructs [1, 2]. Researchers believe that biomimicing normal tissue development is a key to the success of this field and that the function of complex tissue relies on the independent control of macro- and micro-scale features [3–5].

Bio-manufacturing is one area, which aids in creating 3-D tissue scaffolds with complex hierarchical structures capable of biomimicing the structural heterogeneity of the host tissue. Computer-aided rapid-prototyping technologies have been adapted towards the fabrication of 3-D scaffolds with precise spatial and temporal control at the macro- and micro-scale levels [6]. This technology aids designing and manufacturing customized tissue substitutes based on clinical imaging data and computer-aided design (CAD)-based freeform fabrication techniques. Moreover, it allows for the inclusion of vascularization providing nutrient transport and helps create artificial tissue structures

Correspondence: Dr. Wei Sun, Albert Soffa Chair Professor, Department of Mechanical Engineering and Mechanics, Drexel University, Philadelphia, PA 19104, USA
E-mail: sunwei@drexel.edu
Fax: +1-215-895-2094

that closely resemble their *in vivo* state [7, 8]. This technology is applicable not only in engineering tissue substitutes but can also provide sophisticated engineering and manufacturing tools for applications such as drug-evaluations studies and studying fundamental biological problems. A number of biofabrication techniques have been developed such as syringe-based cell deposition for tissue constructs [9–13], inkjet-based cell printing [14–18], laser direct writing of mammalian cells and bacteria, [19–21] and microcontact printing of cell and bacteria [22, 23]. The modified laser-induced forward transfer technique (LIFT) has been used to print pluripotent embryonic carcinoma cells and the study demonstrated near 100% viability as well as retained genotype and phenotype after the printing process [24–27]. In addition, other techniques such as cell manipulation by mechanical, optical, electrical (electrospinning and electrospraying), magnetic, ultrasound, and ionic methods for microfluidics have also been introduced [28–30]. Some new methods have also been added recently such as cell patterning by photo- or electroetching, and soft lithography [31, 32].

Cells are sensitive to environmental changes [33], and therefore when delivered through such systems it is substantially important to understand how the system parameters affect the cell phenotype. For instance, in the case of the bio-printing system, a set of parameters are involved wherein the cells are subjected to combined effects of tension, compression and shear. Nozzle-size variation alters the intensity of shear at the tip and dispensing pressure changes induce compressive or tensile forces on the encapsulated material. From an engineering perspective, these are some of the mechanical cues to which the cells are exposed. Thus, it becomes highly imperative to be able to monitor, control and optimize the process parameters to facilitate the printing cells for fabricating functional tissue. Additionally, development of mathematical models predicting the state of the cell as a function of the shear stresses induced by the system further assists in optimizing the procedure as well as in studying the effects of process-induced mechanical perturbations on cell viability. In our previous study [34], we quantified the live and dead cells using the printing system with various process parameters. Based on the observations from that study, for better controlling the process, it was necessary to analyze and understand the exact state of the cells: whether they were live, injured or necrotic under given conditions. Mechanical trauma leads to necrotic as well as injured cells. Analyzing the cell injury induced by the system would aid in controlling the phenotype of the cell during the process. In addition, developing a model able to determine the shear forces from the system and to predict the live, apoptotic and dead cells from a given set of process parameters further aids in developing tissue constructs using the bioprinting process. This would enable the regulation and control of the cell injury when cells are printed through the system.

This report presents a study that characterizes a multi-nozzle deposition system by assessing and quantifying the degree of cell injury, when encapsulated cells are printed *via* the bio-deposition system. Encapsulated cells were printed at varying dispensing pressures and with different nozzle-tip diameters. The printed cells were then analyzed using apoptosis assays to quantify the live, apoptotic and necrotic cells. An empirical model was developed correlating the process parameters to the induced shear force and predicting the degree of cell damage through the system for a set of process parameters. To capture any morphological changes in the nucleus and membrane induced by the system parameters, the cells were also fluorescently labeled with nuclear and plasma membrane stains.

2 Materials and methods

2.1 Cell printing system

A proprietary solid freeform fabrication-based pressure-driven cell-printing system shown in Fig. 1 has been developed for creating freeform 3-D tissue constructs and for dispensing cells [10, 11]. The system is capable of handling multiple nozzles thereby enabling deposition of multiple cell types, growth factors, or other bioactive compounds in controlled amounts with precise spatial positioning. The cell-printing system operates at room temperature and deposition of the cells and/or biomaterials can be controlled by controlling the dispensing pressure. Geometrical control of the printing pattern is done using in-house developed CAD-driven software. For this study, the pneumatic micro-valve (EFD, East Providence, RI) was used to evaluate cell status under different printing parameters. To study the effects of dispensing pressure and nozzle-tip diameter, the cell-alginate mixture was printed at pressure from 5 to 40 psi using nozzle-tip diameter in the range of 150–400 microns. For each set of parameters, samples were printed of which three samples were analyzed with apoptotic assay immediately after printing. For each parameter, one sample was used to analyze membrane and nuclear damage as well.

Biotechnol. J. 2009, 4, 1168–1177

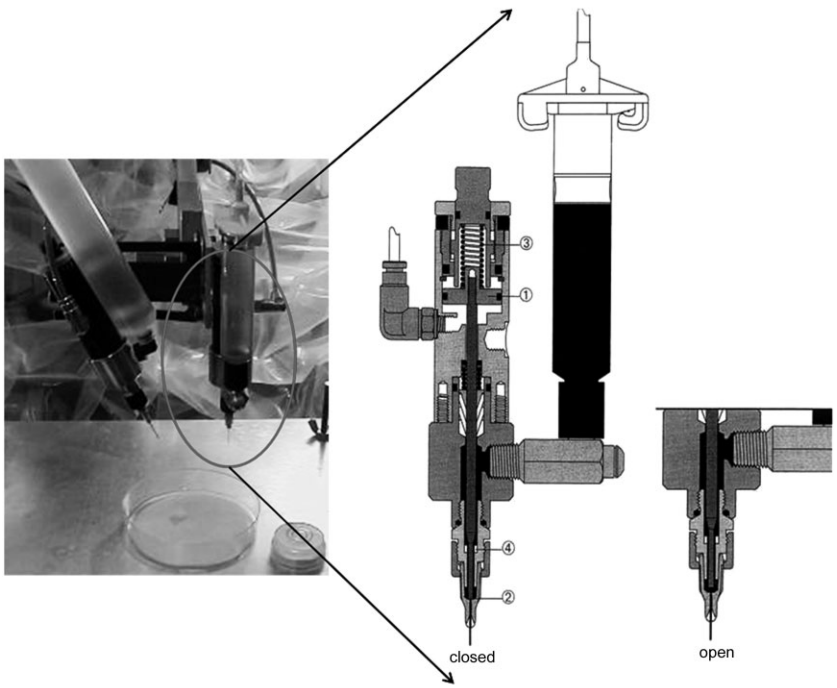

Figure 1. Pressure-driven cell printing system showing closed and open configurations.

2.2 Cell culture and encapsulation

Rat adrenal medulla endothelial RAMEC cells (ATCC, MA) were cultured in DMEM supplemented with 10% fetal bovine serum (FBS), 2 mM L-glutamine, 10 000 IU Penicillin, 10 000 μg/mL Streptomycin and 25 μg/mL Amphotericin-B. They were maintained in the incubator at 5% CO_2 and 37°C. To prepare the polymer solution, medium viscosity sodium alginate powder (Sigma, St. Louis, MO) was dissolved in deionized water as a 1.5% w/v solution. The viscosity of this solution was 490 cP based on our previous study [35]. The alginate solution was sterilized by serial filtration through 0.8, 0.4 and 0.2-micron filters. The cells were gently mixed in viscous sodium alginate solution with Pasteur pipette to ensure a uniform cell distribution. Hemocytometer readings measured the cell concentration at 1×10^6 cells/mL of alginate biopolymer solution. Endothelial cells were chosen because of their usefulness in angiogenesis and potential use in cardiovascular engineering [36].

2.3 Quantifying injury by annexin V

To quantify live, apoptotic and necrotic cells as a function of the mechanical perturbations induced by the process parameters, samples printed implementing each parameter were treated with the annexin V-staining kit (Biovision, Mountain View, CA) following manufacturer's protocol. During early stages of apoptosis the alteration in plasma membrane occurs, resulting into exposure of phophatidylserine (PS) from inner surface to outer surface of the cell membrane [37, 38]. Annexin-V is a protein that specifically binds PS. When used in conjunction with dye measuring membrane integrity (such as propidium iodide, PI), early apoptotic cells (annexin-V positive only) can be distinguished from late apoptotic/necrotic cells (annexin-V and membrane integrity measuring dye positive). Live cells do not bind to any dye, early apoptotic cells bind to annexin-V only, and dead cells bind to both dyes (Vermes *et al*. [38]). The percentages of live, apoptotic and dead necrotic cells were then estimated as described [37]. Briefly, cells from each sample were treated with 5 mL PBS and centrifuged for 10 min to collect the cell pellet for annexin V assay. The cells were resuspended in 500 μL of 1x Binding Buffer and 5 μL of annexin V-FITC and 5 μL of PI were added to each sample. The cell suspension was placed on a glass slide and covered with a glass cover slip. The samples were then viewed under a fluorescence microscope using a dual filter set for FITC & rhodamine. Cell sorting was carried out by the process described elsewhere [37]. From five high-power fields per sample, a minimum of 100 cells were counted from each field. Results were expressed as number of apoptotic, live and necrotic cells per 100 cells. For

each set of process parameters, three samples were analyzed. As a control, unprinted samples (deposited using a pipette) were used.

2.4 Detection of nuclear damage by dual nuclear and membrane stain

To view the morphological alterations in the nucleus and the cell membrane as a function of process parameters, printed samples were counterstained with specific DNA stain Hoechst 33342 and cell-impermeant Alexa Fluor® 594 wheat germ agglutinin (WGA) (Molecular Probes, Invitrogen), which fluoresces nucleus in blue and plasma membrane in red. Fluorescent microscopy was carried out to visualize condensation of nuclear chromatin (pyknosis) and/or nuclear disintegration and dissolution (karyolysis) to estimate the extent and type of cell injury.

2.5 Quantitative model for cell viability prediction from process parameters and induced shear forces

To relate the cell viability to process parameters, a quantitative model was derived from the experimental data. In this approach, the applied dispensing pressure (P) and the nozzle diameter (D) were taken into consideration. The printing system allows for independent adjustments of P and D and therefore they were assumed to be the independent variables in this formulation. A complete second-order model with two independent variables can be expressed as

$$E(y) = \beta_0 + \beta_1 x_1 + \beta_2 x_2 + \beta_3 x_1 x_2 + \beta_4 x_1^2 + \beta_5 x_2^2 \quad (1)$$

where, $E(y)$ is the expected value (the mean value) for percentage of live cells (P_L), percentage of injured cells (P_I), and percentage of dead cells (P_D); x_1 and x_2 represent the independent variables nozzle diameter and pressure. The constants β_0 through β_5 were derived by correlating the experimental data wherein percentages of live, apoptotic and dead cells were determined for a range of process parameters.

During the printing process, cells suspended in the alginate solution also experienced shear stress that was induced by the applied pressure. Multitude parameters affect the maximum shear stress, including the pressure applied, nozzle size, alginate concentration etc. An analytic model for predicting the maximum shear stress in the nozzle has been developed assuming the alginate aqueous solution to be a non-Newtonian fluid [35]. The model correlates the printing-process parameters to the maximum shear stress in the system. In this study, the model was extended to predict cell viability as a function of maximum shear stress in the system. For the sake of completeness, the model is outlined as follows. For a non-Newtonian fluid, the relationship of shear stress τ and the apparent shear rate γ can be represented by the power-law function as shown in Eq. (2):

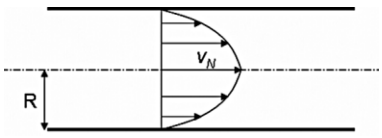

Figure 2. Schematic of fluid velocity through the cross-section of a capillary or nozzle tip.

$$\tau = \eta\dot{\gamma} = K\dot{\gamma}^n \quad (2)$$

where η is the viscosity, γ is the shear rate, constant K is the consistency index, and the constant n is the power law index. Figure 2 shows schematic of fluid velocity through the cross-section of a capillary or a nozzle tip. Here, the wall shear rate can be expressed as

$$\gamma = \frac{v_N}{R} \quad (3)$$

where v_N is the deposition speed, R is the nozzle radius. On the other hand, based on the principle of mass conservation, the deposition speed v_N is related to the deposition flow rate Q as

$$v_N = \frac{Q}{\pi R^2} \quad (4)$$

The relationship between the flow rate Q and the process and material parameters is derived by generalizing Poiseuille's equation for predicting the flow rate of a non-Newtonian cell-hydrogel extruded from the bio-deposition system. For an incompressible non-Newtonian fluid, the flow through a uniform circular cross-section can be expressed as

$$\left(\frac{\partial v}{\partial r}\right)^n = \frac{r\dot{\gamma}_0^{n-1}}{2\eta_0}\frac{\partial P}{\partial z} \quad (5)$$

where, η_0 is the limited viscosity as low shear rates and γ_0 is the corresponding shear rate. The above equation can be integrated between limits $v = v$ at radius r and $v = 0$ at radius R to give

$$v = \left(\frac{n}{n+1}\right)\dot{\gamma}_0^{\frac{n-1}{n}}\left(\frac{\partial P/\partial z}{2\eta_0}\right)^{1/n}\left(r^{\frac{n+1}{n}} - R^{\frac{n+1}{n}}\right) \quad (6)$$

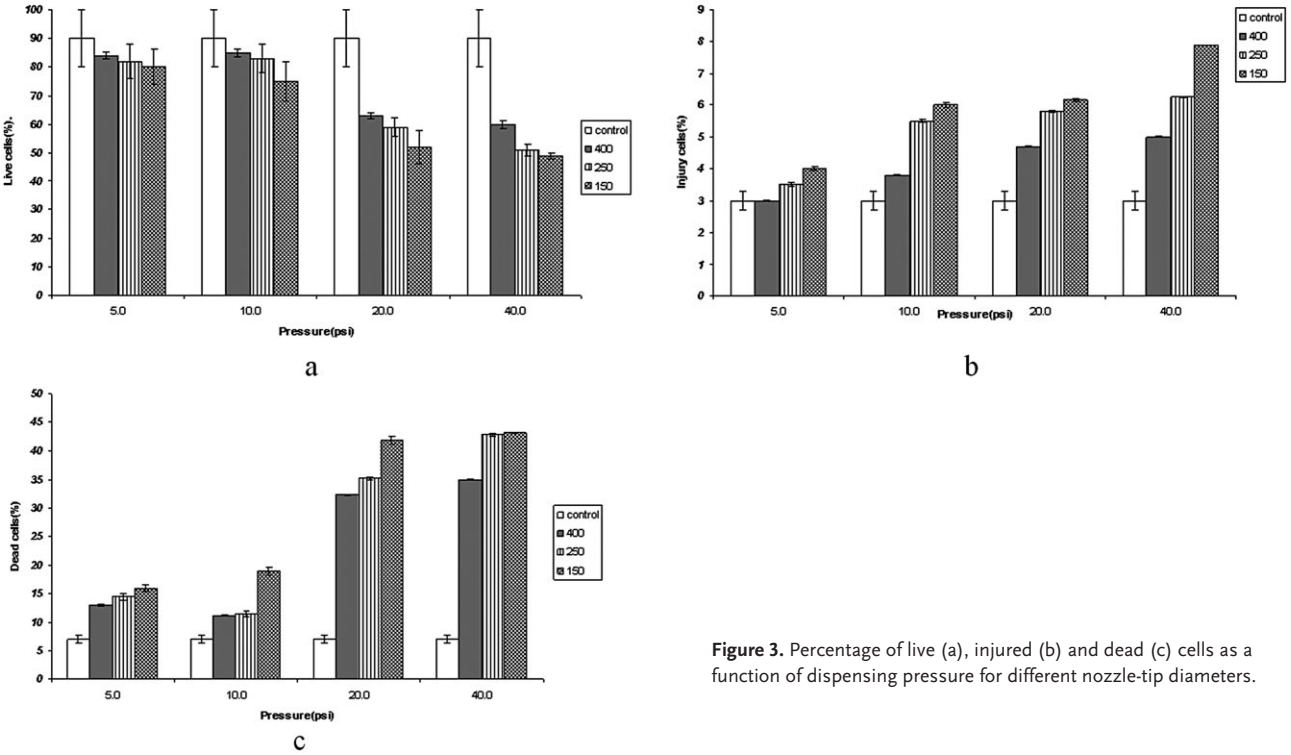

Figure 3. Percentage of live (a), injured (b) and dead (c) cells as a function of dispensing pressure for different nozzle-tip diameters.

The volume flow rate can then be determined by

$$Q = \int_0^R 2\pi r v dr = \int_0^R 2\pi r v_0 \left(1 - \left(\frac{r}{R}\right)^{\frac{n+1}{n}}\right) dr \qquad (7)$$

$$= \left(\frac{n}{3n+1}\right)\pi\gamma_0^{\frac{n-1}{n}}\left(\frac{\partial P/\partial z}{2\eta_0}\right)^{1/n} R^{\frac{3n+1}{n}}$$

Note that the power-law index n and consistency index K are determined experimentally via measured apparent viscosity and corresponding shear rate. K and n can then be used in Eq. (7) to predict the flow rate Q. From Eqs. (2–4, and 7), the maximum shear stress at the wall is thus given as

$$\tau_{\max} = K\left(\frac{8Q}{\pi D^3}\right)^n = K\left(\frac{n}{3n+1}\right)^n \dot{\gamma}_0^{(n-1)} \frac{D}{2}\left(\frac{\partial P/\partial z}{2\eta_0}\right) \qquad (8)$$

$$= \left(\frac{n}{3n+1}\right)^n \frac{D}{4}\frac{\partial P}{\partial z}$$

Here, the pressure gradient $\partial P/\partial z$ is a unique value for a given deposition system and is a function of the nozzle diameter, pressure applied, and the internal geometry of the whole valve system. Combining the quantitative model for cell viability and process parameters along with the shear stress model, a predictive curve can be established to determine the percentage of live cells for a set of process parameters and when subjected to a particular shear stress.

2.6 Statistical analysis

The statistical significance of experimental data was determined by two-way analysis of variance (ANOVA) since the study incorporated effects of two independent variables, dispensing pressure and nozzle diameter. The paired wise test was combined with the Tukey post-hoc test at the significance level of less than 0.05 ($p < 0.05$) using SPSS® version 15 for Windows® software package.

3 Results

3.1 Effect of dispensing pressure and nozzle size on cell viability: Experimental

A set of parametric experimental studies were conducted to assess the effect of the dispensing pressure and the nozzle size on the viability of cells. Each data point was an average of five representative live, apoptotic and necrotic images for each sample. Analysis was first performed by segregating the samples into three experimental groups ac-

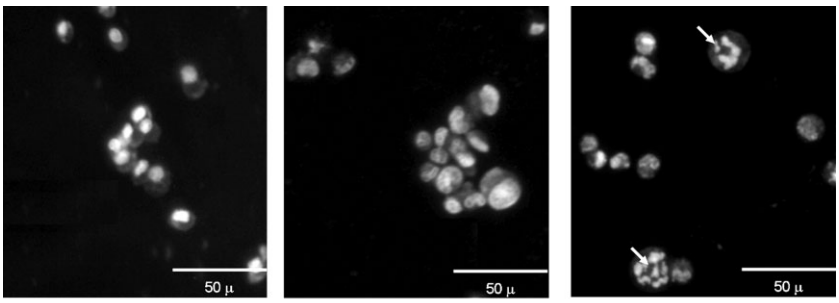

Figure 4. Samples counterstained with DNA stain Hoechst 33342 and cell-impermeant Alexa Fluor ® 594 wheat germ agglutinin (WGA). (a) Unprinted. (b) Samples printed at 5 psi with 400-micron nozzle. (c) Samples printed at 40 psi with 150-micron nozzle, indicating pyknosis and karyolysis (indicated by arrows).

cording to different nozzle diameters of 150, 250, and 400 microns. For each nozzle diameter, the dispensing pressures were varied and studied at 5, 10, 20, and 40 psi. Figure 3a indicates the decrease in percentage of live cells with increasing dispensing pressure and decreasing nozzle-tip diameter. Figures 3b and 3c indicate the increase in percentage of injured and necrotic cells with increasing dispensing pressure and decreasing nozzle-tip diameter. It can be seen that the effect of pressure is significantly larger than the effect of the nozzle diameter. At higher pressures, there is an increase in the number of injured cells as well as necrotic cells.

The DNA stain along with the membrane stain allows for visualizing the morphological changes in the samples. Compared to the control samples and samples printed under moderate process parameters (400-micron nozzle-tip diameter and dispensing pressure of 5 psi), samples exposed to extreme conditions (nozzle tip diameter of 150 microns and high dispensing pressure of 40 psi) indicated pyknosis as well as karyolysis (Figs. 4a–c).

3.2 Effect of dispensing pressure and nozzle size on cell viability: Modeling

An empirical model has been developed to predict the percentage of live (P_L), injured (P_I) and dead cells (P_D) as a function of dispensing pressure and nozzle-tip diameter. Figure 5 indicates the predicted P_L, P_I and P_D as functions of the pressure and the nozzle diameters. The equations predicting the percentage of live, apoptotic and necrotic cells expressed as a function of dispensing pressure and nozzle diameter are as follows

$$E(P_L) = 0.8563 + 0.655x_1 - 0.0268x_2 + 0.0061x_1x_2 - 0.76x_1^2 + 0.000352x_2^2 \quad (9)$$

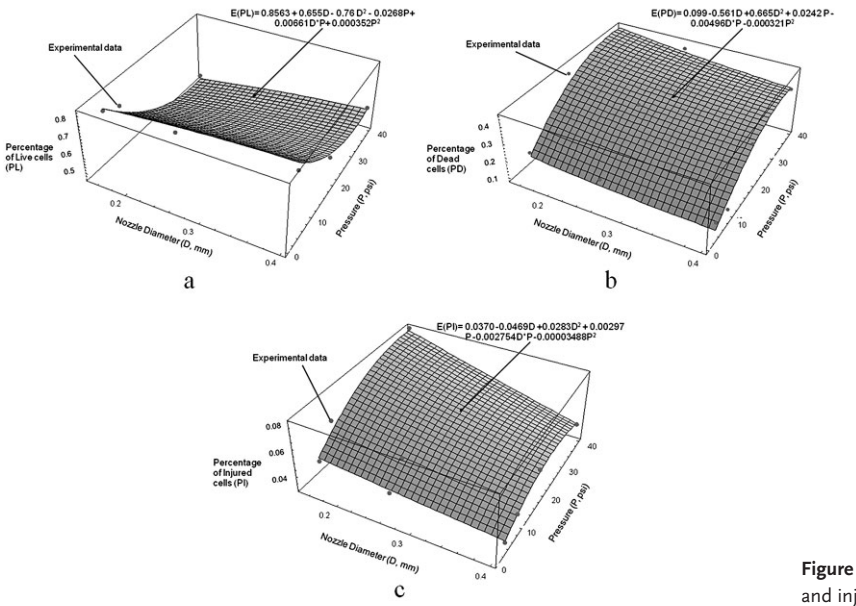

Figure 5. Surface plot for percentage of live (a), dead (b) and injured (c) cells as a function of process parameters.

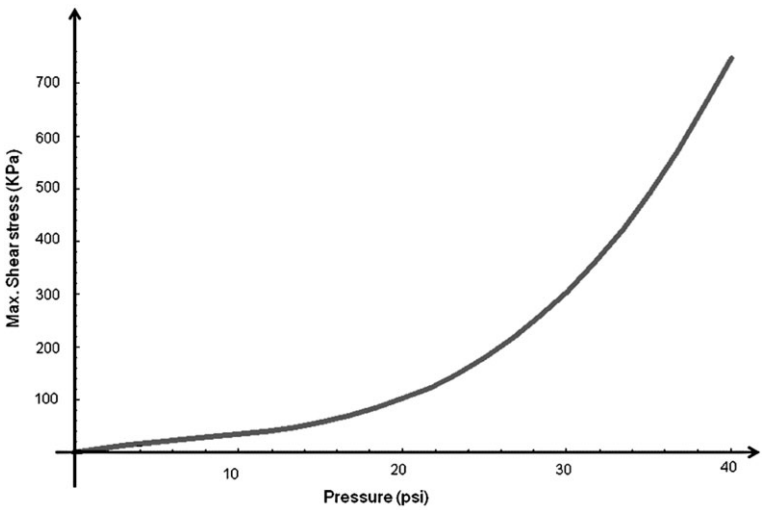

Figure 6. Maximum shear stress *vs.* dispensing pressure for nozzle-tip diameter of 250 microns.

$$E(P_I) = 0.037 - 0.0469x_1 + 0.00297x_2 - 0.002754x_1x_2 - 0.00003488x_1^2 + 0.0283x_2^2 \quad (10)$$

$$E(P_D) = 0.099 - 0.561x_1 + 0.0242x_2 - 0.00496x_1x_2 + 0.665x_1^2 - 0.000321x_2^2 \quad (11).$$

A second quantitative model is implemented to correlate the process parameters to the maximum shear force in the system. This mathematical model enables to effectively correlate the cell viability to process parameters and induced shear forces. Figure 6 shows the predicted non-linear increase in maximum shear force with increasing pressure for a nozzle-tip diameter of 250 microns.

As indicated in previous sections, the percentages of live, injured, and dead cells, denoted as P_L, P_I and P_D, respectively, were determined through image analysis for all test samples and statistical analyses were performed. Assuming that P_L, P_I and P_D for a given condition follow the normal distribution, the mean values and SD can be determined. Figure 7 depicts probability distributions of P_L for test samples with 150-micron nozzle diameter. The shift in the curve clearly indicates significant effect of pressure on cell viability. As seen in the figure there is a decrease of 6.25% in the percentage of live cells at 10 psi and 150 microns compared to the cells dispensed at 5 psi with the same nozzle. Similarly, the percentage of cells was reduced significantly by 38.75% when constructs were printed at 40 psi compared to those printed at 5 psi. The trends were similar when the nozzle sizes were changed to 250 as well as 400 microns. At low pressures (5 psi), the cell viability through a 150-micron nozzle was reduced to 4.76% as compared to the cell viability through a 400-micron nozzle.

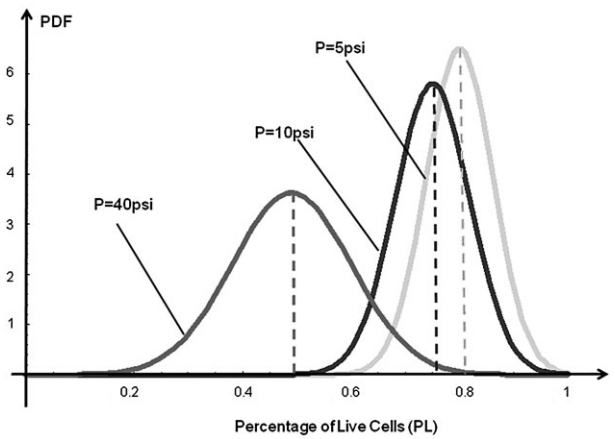

Figure 7. Probability density plot of percentage of live cells with cells printed using 150-micron nozzle-tip diameter at pressure of 5, 10 and 40 psi.

Combining the surface model with the shear stress model enables to effectively predict the cell viability as a function of the maximum shear force induced by the process. Figure 8 indicates the percentage decrease in cell viability with increasing shear stress.

4 Discussion

Normal cells respond to stress and injurious stimuli by undergoing adaptation. Cells that are unable to adapt undergo cell injury followed by cell death. Cell injury can be reversible wherein normal homeostasis is restored or irreversible wherein cells die. This study focuses on characterizing cell viability as well as injury induced by the bioprinting system. One can observe from Figs. 3a–c that

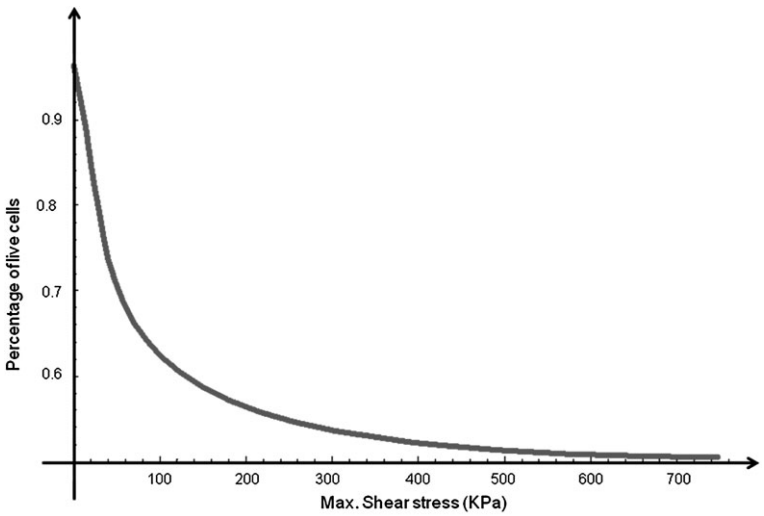

Figure 8. Percentage cell viability *vs.* maximum shear stress.

cell viability varies with dispensing pressure and nozzle diameter. The cell viability decreases as the pressure increases and the nozzle diameter decreases. It is seen that the effect of pressure is significantly larger than the effect of the nozzle diameter. At higher pressures, there is an increase in the number of apoptotic cells as well as necrotic cells. It is interesting to note that in all the different scenarios the number of apoptotic cells is less than 10%. This could be due to the severity of damage especially caused at high pressures directly leading to cell death. Moreover, it can be observed that the degree of cell damage is higher due to effects of pressure rather than effects of the nozzle-tip diameter. Statistical analysis proved that all the average numbers representing the percentage of live, dead and apoptotic cells taking into account the combined effects of pressure and nozzle diameter were significantly different at statistically significant level p <0.05. In addition, the morphological changes in the nucleus due to variations in pressure and nozzle-tip diameter are clearly visible in Fig. 4. High dispensing pressure and small nozzle diameter lead to pyknosis and karyolysis that lead to cell death and low cell viability whereas printing at lower dispensing pressures and using larger nozzle diameters do not show any visible morphological damage to the nucleus. Clearly, high pressure and small nozzle diameters induce more damage to the cells as reflected quantitatively in the annexin V kit and qualitatively in the DNA staining. However, it must be noted that this study was conducted to analyze and characterize the cells immediately after printing, and therefore, long-term effects of injury or cell recovery have not been taken into consideration.

The surface-fitting model along with the shear stress model allows for further correlating the degree of cell damage to the process parameters and induced shear stress. As seen in Figs. 5a–c, the effects of dispensing pressure are more significant on cell viability than the varying nozzle diameter. In addition, the synergistic effects of both dispensing pressure and nozzle diameter significantly affect the percentage of live, apoptotic and dead cells. From Fig. 8 it can be observed that higher stress leads to lower cell viability as expected. For instance, while using a 250-microns nozzle tip, the cell viability through the system reduces to less than 50% when the maximum shear stress increases beyond 150 kPa. This indicates that the damage caused at such shear stresses is irreversible and leads to cell death. The current model takes into account the two process parameters, dispensing pressure and nozzle tip diameter. Other parameters such as alginate concentration have previously been optimized for cell viability as well as structural integrity [10, 11]. Furthermore, the model takes into account the maximum shear force within the system. The effect of time duration of printing on cell viability is assumed minimal, since the printing process was completed in 15 min. Although this modeling technique allows for better control and monitors the state of the cell within the system, the forces at the cellular microenvironment have not been characterized. Future studies should include a computational fluid dynamics model to accurately characterize the cellular microenvironment as a function of the process parameters in the printing system.

Though using low pressures and bigger nozzle tips is favorable for cell printing, it is important to take into consideration the drawbacks of using

such process parameters as well. For instance, while using larger nozzle tips the structures that are produced are invariably going to be larger in dimensions. However, this characterization study enables parameter optimization to produce constructs of required dimension with minimum degree of damage. For example, in order to produce constructs in the range of 150 microns the dispensing pressure should be set to 5–10 psi. In addition, the system is capable of printing smaller structures (~50 microns); however it must be done at low dispensing pressures. It should also be noted that the data are specific to endothelial cells and are likely to change when different cell types are used in the system. While the focus of this study has been to optimize the process parameters to minimize cell injury at the time of printing, it must be noted that it does not attempt to explain effects of process parameters on cell function especially over longer periods.

In this study, the multi-nozzle cell printing system has been characterized and optimized by assessing and quantifying the degree of cell apoptosis, when encapsulated endothelial cells are printed via the bio-deposition system. This study enables us to quantify the degree of cell damage resulting from implementing different sets of process parameters using an apoptosis assay. Specifically the effects of dispensing pressure and nozzle diameters on cell injury have been quantified and studied.

In addition, a mathematical model has been developed correlating the process parameters to the induced shear force and predicting the degree of cell damage through the system. Relating the process parameters to the maximum shear stress in the system and further correlating it to predict cell viability allows us to better control and regulate cell damage through the process. This study provides a scientific basis for characterizing and optimizing bioprinting processes in the area of biomanufacturing of functional tissue constructs. Future work will include analyzing the function and phenotype of the cells when using different sets of printing parameters. Studies will also be conducted to observe changes in cell behavior over longer time periods.

The authors would like to acknowledge the support from NSF grant NSF-0700405 towards this research.

The authors have declared no conflict of interest.

5 References

[1] Griffith, L. G., Swartz, M. A., Capturing complex 3D tissue physiology *in vitro*. *Nat. Rev. Mol. Cell. Biol.* 2006, *7*, 211–224.

[2] Langer, R. S., Vacanti, J. P., Tissue engineering: the challenges ahead. *Scientific American* 1999, *280*, 86–89.

[3] Ghosh, K., Ingber, D. E., Micromechanical control of cell and tissue development: Implications for tissue engineering. *Adv. Drug Deliv. Rev.* 2007, *59*, 1306–1318.

[4] Ingber, D. E., Mow, V. C., Butler, D., Niklason, L. *et al.*, Tissue engineering and developmental biology: going biomimetic. *Tissue Eng.* 2006, *12*, 3265–3283.

[5] Lauffenburger, D. A., Griffith, L. G., Who's got pull around here? Cell organization in development and tissue engineering. *Proc. Natl. Acad. Sci. USA* 2001, *98*, 4282–4284.

[6] Chen, A. A., Tsang, V. L., Albrecht, D. R., Bhatia, S. N., 3-D Fabrication technology for tissue engineering, *BioMEMS Biomed. Nanotechnol.* 2007, pp. 23–38.

[7] Chu, T. M., Hollister, S. J., Halloran, J. W., Feinberg, S. E., Orton, D. G., Manufacturing and characterization of 3-d hydroxyapatite bone tissue engineering scaffolds. *Ann. NY Acad. Sci.* 2002, *961*, 114–117.

[8] Zeltinger, J., Sherwood, J. K., Graham, D. A., Mueller, R., Griffith, L. G., Effect of pore size and void fraction on cellular adhesion, proliferation, and matrix deposition. *Tissue Eng.* 2001, *7*, 557–572.

[9] Ang, T. H., Sultana, F. S. A., Hutmacher, D. W., Wong, Y. S. *et al.*, Fabrication of 3D chitosan–hydroxyapatite scaffolds using a robotic dispensing system. *Mat. Sci. Eng. C* 2002, *20*, 35–42.

[10] Khalil, S., Nam, J., Sun, W., Multi-nozzle deposition for construction of 3D biopolymer tissue scaffolds. *Rapid Prototyping J.* 2005, *11*, 9–17.

[11] Khalil, S., Sun, W., Biopolymer deposition for freeform fabrication of hydrogel tissue constructs. *Mat. Sci. Eng. C* 2007, *27*, 469–478.

[12] Landers, R., Mülhaupt, R., Desktop manufacturing of complex objects, prototypes and biomedical scaffolds by means of computer-assisted design combined with computer-guided 3D plotting of polymers and reactive oligomers. *Macromol. Mat. Eng.* 2000, *282*, 17–21.

[13] Yan, Y., Xiong, Z., Hu, Y., Wang, S. *et al.*, Layered manufacturing of tissue engineering scaffolds via multi-nozzle deposition. *Mat. Lett.* 2003, *57*, 2623–2628.

[14] Boland, T., Mironov, V., Gutowska, A., Roth, E. A., Markwald, R. R., Cell and organ printing 2: Fusion of cell aggregates in three-dimensional gels. *Anatom. Rec. Part A: Discov. Mol. Cell. Evol. Biol.* 2003, *272A*, 497–502.

[15] Mironov, V., Markwald, R. R., Forgacs, G., Organ printing: self-assembling cell aggregates as „BIOINK". *Sci. Med.* 2003, *9*, 69–71.

[16] Varghese, D., Deshpande, M., Xu, T., Kesari, P. *et al.*, Advances in tissue engineering: Cell printing. *J. Thor. Cardiovasc. Surg.* 2005, *129*, 470–472.

[17] Xu, T., Gregory, C. A., Molnar, P., Cui, X. *et al.*, Viability and electrophysiology of neural cell structures generated by the inkjet printing method. *Biomaterials* 2006, *27*, 3580–3588.

[18] Xu, T., Jin, J., Gregory, C., Hickman, J. J., Boland, T., Inkjet printing of viable mammalian cells. *Biomaterials* 2005, *26*, 93–99.

[19] Barron, J. A., Ringeisen, B. R., Kim, H., Spargo, B. J., Chrisey, D. B., Application of laser printing to mammalian cells. *Thin Solid Films* 2004, *453–454*, 383–387.

[20] Odde, D. J., Renn, M. J., Laser-guided direct writing for applications in biotechnology. *Trends Biotechnol.* 1999, *17*, 385–389.
[21] Wu, P. K., Ringeisen, B. R., Callahan, J., Brooks, M. *et al.*, The deposition, structure, pattern deposition, and activity of biomaterial thin-films by matrix-assisted pulsed-laser evaporation (MAPLE) and MAPLE direct write. *Thin Solid Films* 2001, *398–399*, 607–614.
[22] Stevens, M. M., Mayer, M., Anderson, D. G., Weibel, D. B. *et al.*, Direct patterning of mammalian cells onto porous tissue engineering substrates using agarose stamps. *Biomaterials* 2005, *26*, 7636–7641.
[23] Weibel, D. B., Lee, A., Mayer, M., Brady, S. F. *et al.*, Bacterial printing press that regenerates its ink: contact-printing bacteria using hydrogel stamps. *Langmuir* 2005 *21*, 6436–6442.
[24] Barron, J. A., Krizman, D. B., Ringeisen, B. R., Laser printing of single cells: Statistical analysis, cell viability, and stress. *Ann. Biomed. Eng.* 2005, *33*, 121–130.
[25] Barron, J. A., Wu, P., Ladouceur, H. D., Ringeisen, B. R., Biological laser printing: A novel technique for creating heterogeneous 3-dimensional cell patterns. *Biomed. Microdevices* 2004, *6*, 139–147.
[26] Chen, C. Y., Barron, J. A., Ringeisen, B. R., Cell patterning without chemical surface modification: Cell–cell interactions between printed bovine aortic endothelial cells (BAEC) on a homogeneous cell-adherent hydrogel. *Appl. Surf. Sci.* 2006 *252*, 8641–8645.
[27] Ringeisen, B. R., Kim, H., Barron, J. A., Krizman, D..B. *et al.*, Laser printing of pluripotent embryonal carcinoma cells. *Tissue Eng.* 2004, *10*, 483–491.
[28] Patrick, K., Odenwälder, S. I., McEwan, J. R., Jayasinghe, S. N., Bio-electrosprays: A novel electrified jetting methodology for the safe handling and deployment of primary living organisms. *Biotechnol. J.* 2007, *2*, 622–630.
[29] Townsend-Nicholson, A., Jayasinghe, S. N., Cell electrospinning: a unique biotechnique for encapsulating living organisms for generating active biological microthreads/scaffolds. *Biomacromolecules* 2006, *7*, 3364–3369.
[30] Yi, C., Li, C.-W., Ji, S., Yang, M., Microfluidics technology for manipulation and analysis of biological cells. *Analytica Chimica Acta* 2006, *560*, 1–23.
[31] Albrecht, D. R., Tsang, V. L., Sah, R. L., Bhatia, S. N., Photo and electropatterning of hydrogel encapsulated living cell arrays. *Lab Chip* 2005, *5*, 111–118.
[32] Kane, R. S., Takayama, S., Ostuni, E., Ingber, D. E., Whitesides, G. M., Patterning proteins and cells using soft lithography. *Biomaterials* 1999, *20*, 2363–2376.
[33] Wong, J. Y., Leach, J. B., Brown, X. Q., Balance of chemistry, topography, and mechanics at the cell-biomaterial interface: Issues and challenges for assessing the role of substrate mechanics on cell response. *Surf. Sci.* 2004, *570*, 119–133.
[34] Chang, R., Nam, J., Sun, W., Effects of dispensing pressure and nozzle diameter on cell survival from solid freeform fabrication-based direct cell writing. *Tissue Eng. Part A.* 2008, *14*, 41–48.
[35] Khalil, S., Deposition and structural formation of 3D alginate tissue scaffolds, Ph.D Thesis, Drexel University, Philadelphia, PA, 2006.
[36] Bader, A., Schilling, T., Teebken, O. E., Brandes, G. *et al.*, Tissue engineering of heart valves-human endothelial cell seeding of detergent acellularized porcine valves. *Eur. J. Cardio-Thor. Surg.* 1998, *14*, 279–284.
[37] Shounan, Y., Feng, X., O'Connell, P. J., Apoptosis detection by annexin V binding: a novel method for the quantitation of cell-mediated cytotoxicity. *J. Immunol. Methods* 1998, *217*, 61–70.
[38] Vermes, I., Haanen, C., Steffens-Nakken, H., Reutellingsperger, C., A novel assay for apoptosis flow cytometric detection of phosphatidylserine expression on early apoptotic cells using fluorescein labelled Annexin V. *J. Immunol. Methods* 1995, *184*, 39–51.

